Available online at www.sciencedirect.com
SCIENCE DIRECT®
International Journal of Heat and Mass Transfer 49 (2006) 132–143
International Journal of HEAT and MASS TRANSFER
www.elsevier.com/locate/ijhmt

Simultaneous heat and mass transfer characteristics for wavy fin-and-tube heat exchangers under dehumidifying conditions

Worachest Pirompugd [a], Somchai Wongwises [a,*], Chi-Chuan Wang [b]

[a] *Fluid Mechanics, Thermal Engineering and Multiphase Flow Research Laboratory (FUTURE), Department of Mechanical Engineering, King Mongkut's University of Technology Thonburi, Bangmod, Bangkok 10140, Thailand*

[b] *Energy and Resources Laboratory, Industrial Technology Research Institute, Hsinchu 310, Taiwan, ROC*

Received 3 February 2005; received in revised form 8 May 2005
Available online 3 October 2005

Abstract

The present study proposes a new reduction method to calculate the heat and mass transfer characteristics of the wavy fin-and-tube heat exchangers under dehumidifying conditions. For fully wet conditions, the sensible heat transfer and mass transfer characteristics are relatively insensitive to the inlet relative humidity. The heat and mass transfer performances show appreciable influence of fin spacing at 1-row configuration. Both the heat and mass transfer performances increase when the fin spacing is reduced. However, the difference becomes less noticeable when $Re_{Dc} > 3000$. For 1-row configuration, larger wave height shows much larger difference with the fin spacing. However, the effect of inlet conditions and geometrical parameters on the heat and mass performance becomes less significant with the rise of number of tube rows. Test results show that the heat and mass transfer analogy is roughly applicable (the ratios of $h_{c,o}/h_{d,o}C_{p,a}$ are in the range 0.6–1.1, and is insensitive to change of fin spacing). The correlations are proposed to describe the heat and mass transfer characteristics. These correlations can describe 94.19% of the j_h factors within 15% and 83.72% of the j_m factors within 15%. Correspondingly, 93.02% of the ratios of $h_{c,o}/h_{d,o}C_{p,a}$ are predicted by the proposed correlation within 15%.

Keywords: Wavy fin-and-tube heat exchangers; Dehumidifying; Heat transfer; Mass transfer

1. Introduction

The plate fin-and-tube heat exchangers are the most widely used heat exchangers in association with the application of air-conditioning and refrigeration systems. The heat exchangers can be used for condensers where surface is dry and evaporators in which surface may be wet provided the fin temperature is below the dew point temperature. In regard to the wet surface, simultaneous heat and mass transfer occurs along the fin surfaces. In general, the complexity of the moist air flow pattern across the fin-and-tube heat exchangers under dehumidifying conditions makes the theoretical

* Corresponding author. Tel.: +66 2 470 9115; fax: +66 2 470 9111.
E-mail address: somchai.won@kmutt.ac.th (S. Wongwises).

0017-9310/$ - see front matter © 2005 Elsevier Ltd. All rights reserved.
doi:10.1016/j.ijheatmasstransfer.2005.05.043

Nomenclature

A_f	surface area of fin, m^2
A_0	total surface area, m^2
$A_{p,i}$	inside surface area of tubes, m^2
$A_{p,o}$	outside surface area of tubes, m^2
b'_p	slope of the air saturation curved between the outside and inside tube wall temperature, J kg^{-1} K^{-1}
b'_r	slope of the air saturation curved between the mean water temperature and the inside wall temperature, J kg^{-1} K^{-1}
$b'_{w,m}$	slope of the air saturation curved at the mean water film temperature of the fin surface, J kg^{-1} K^{-1}
$b'_{w,p}$	slope of the air saturation curved at the mean water film temperature of the tube surface, J kg^{-1} K^{-1}
$C_{p,a}$	moist air specific heat at constant pressure, J kg^{-1} K^{-1}
$C_{p,w}$	water specific heat at constant pressure, J kg^{-1} K^{-1}
D_c	tube outside diameter (include collar), m
D_i	tube inside diameter, m
f_i	in-tube friction factors of water
F	correction factor
G_{max}	maximum mass velocity based on minimum flow area, kg m^{-2} s^{-1}
$h_{c,o}$	sensible heat transfer coefficient, W m^{-2} K^{-1}
$h_{d,o}$	mass transfer coefficient, kg m^{-2} K^{-1}
h_i	inside heat transfer coefficient, W m^{-2} K^{-1}
$h_{o,w}$	total heat transfer coefficient for wet external fin, W m^{-2} K^{-1}
I_0	modified Bessel function solution of the first kind, order 0
I_1	modified Bessel function solution of the first kind, order 1
i	enthalpy, kJ kg^{-1}
i_a	air enthalpy , kJ kg^{-1}
$i_{a,in}$	inlet air enthalpy, kJ kg^{-1}
$i_{a,m}$	mean air enthalpy, kJ kg^{-1}
$i_{a,out}$	outlet air enthalpy, kJ kg^{-1}
i_g	saturated water vapor enthalpy, kJ kg^{-1}
i_m	mean enthalpy, kJ kg^{-1}
$i_{r,in}$	saturated air enthalpy at the inlet water temperature, kJ kg^{-1}
$i_{r,m}$	mean saturated air enthalpy at the mean water temperature, kJ kg^{-1}
$i_{r,out}$	saturated air enthalpy at the outlet water temperature, kJ kg^{-1}
$i_{s,fm}$	saturated air enthalpy at the fin mean temperature, kJ kg^{-1}
$i_{s,fb}$	saturated air enthalpy at the fin base temperature, kJ kg^{-1}
$i_{s,p,i,m}$	mean saturated air enthalpy at the mean inside tube wall temperature, kJ kg^{-1}
$i_{s,p,o,m}$	mean saturated air enthalpy at the mean outside tube wall temperature, kJ kg^{-1}
$i_{s,w}$	saturated air enthalpy at the water film temperature, kJ kg^{-1}
$i_{s,w,m}$	mean saturated air enthalpy at the mean water film temperature of the fin surface, kJ kg^{-1}
j_h	Chilton–Colburn j-factor of the heat transfer
j_m	Chilton–Colburn j-factor of the mass transfer
K_0	modified Bessel function solution of the second kind, order 0
K_1	modified Bessel function solution of the second kind, order 1
k_f	thermal conductivity of fin, W $m^{-1}K^{-1}$
k_i	thermal conductivity of water, W $m^{-1}K^{-1}$
k_p	thermal conductivity of tube, W $m^{-1}K^{-1}$
k_w	thermal conductivity of water film, W $m^{-1}K^{-1}$
L_p	tube length, m
$\dot{m}_a$	air mass flow rate, kg s^{-1}
$\dot{m}_w$	water mass flow rate, kg s^{-1}
N	number of tube rows
P	pressure, Pa
P_d	wave height, m
P_l	longitudinal tube pitch, m
Pr	Prandtl number
P_t	transverse tube pitch, m
$\dot{Q}$	heat transfer rate, W
$\dot{Q}_a$	air side heat transfer rate, W
$\dot{Q}_{avg}$	average heat transfer rate, W
$\dot{Q}_{total}$	total heat transfer rate, W
$\dot{Q}_w$	water side heat transfer rate, W
R	ratio of heat transfer characteristic to mass transfer characteristic
RH	relative humidity
r_i	distance from the center of the tube to the fin base, m
r_o	distance from the center of the tube to the fin tip, m
Re_{Di}	Reynolds number based on inside diameter
Re_{Dc}	Reynolds number based on outside diameter (include collar)
Sc	Schmidt number
Sp	fin spacing, m
T_a	air temperature, K
T_w	water temperature, K
$T_{w,m}$	mean temperature of the water film, K
$T_{p,i,m}$	mean temperature of the inner tube wall, K

$T_{p,o,m}$	mean temperature of the outer tube wall, K	$W_{s,w}$	saturated air humidity ratio at the water film temperature, kg kg^{-1}
$T_{r,m}$	mean temperature of water, K	$W_{s,w,m}$	mean saturated air humidity ratio at the mean water film temperature of the fin surface, kg kg^{-1}
t	fin thickness, m	X_f	projected fin length, m
$U_{o,w}$	wet surface overall heat transfer coefficient, based on enthalpy difference, kg m^{-2}s^{-1}	y_w	thickness of condensate water film, m
V	average velocity, m s^{-1}	ε	fin factor
W_a	humidity ratio of moist air, kg kg^{-1}	$\eta_{f,wet}$	wet fin efficiency
$W_{a,m}$	mean air humidity ratio, kg kg^{-1}	μ	dynamic viscosity, N s m^{-2}
$W_{s,p,o,m}$	mean saturated air humidity ratio at the mean outside tube wall temperature, kg kg^{-1}	ρ	mass density, kg m^{-3}

simulations very difficult. Hence, most of the published work is resorted to experimentation.

For better improvement of the overall performance of fin-and-tube heat exchangers, the fin surface can be in the form of enhanced surfaces such as wavy, louver, and slit. The wavy fin surface is one of the most popular surfaces for it can lengthen the flow path and disturb the air flow without considerable increase of pressure drop. The air-side performance of wavy fin-and-tube heat exchanger had been studied by many researchers [1–7]. Even though many efforts have been devoted to the study of the wet-coils, the available literature on the dehumidifying heat exchangers still offers limited information to assist the designer in sizing and rating a fin-and-tube heat exchanger. This can be made clear from the reported data were mainly focused on the study of the sensible heat transfer characteristics, little attention was paid to the mass transfer characteristics. Therefore, the objective of the present study is to provide further systematic experimental information relevant to the mass transfer performance and propose a new reduction method to determine the air-side performance of fin-and-tube heat exchangers under dehumidifying conditions. The effects of inlet relative humidity, fin spacing, and the number of tube rows on the mass transfer characteristics are examined in this study.

2. Experimental apparatus

The schematic diagram of the experimental air circuit assembly is shown in Fig. 1. It consists of a closed-loop wind tunnel in which air is circulated by a variable speed centrifugal fan (7.46 kW, 10 HP). The air duct is made of galvanized sheet steel and has an 850 mm × 550 mm cross-section. The dry-bulb and wet-bulb temperatures of the inlet air are controlled by an air-ventilator that can provide a cooling capacity up to 21.12 kW (6RT). The air flow-rate measurement station is an outlet chamber setup with multiple nozzles. This setup is based on the ASHRAE 41.2 standard [8]. A differential pressure transducer is used to measure the pressure difference

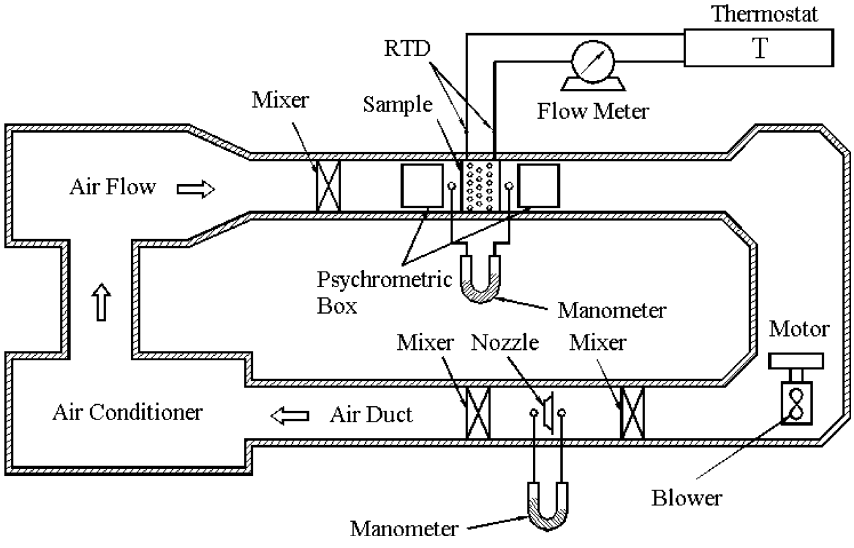

Fig. 1. Schematic of experimental set-up.

across the nozzles. The air temperatures at the inlet and exit zones across the sample heat exchangers are measured by two psychrometric boxes based on the ASHRAE 41.1 standard [9].

The working medium or the tube side is cold water. A thermostatically controlled reservoir provides the cold water at selected temperatures. The temperature differences on the water side are measured by two precalibrated RTDs. The water volumetric flow rate is measured by a magnetic flow meter with a ±0.001 L/s precision. All the temperature measuring probes are resistance temperature devices (Pt100), with a calibrated accuracy of ±0.05 °C. In the experiments, only the data that satisfy the ASHRAE 33-78 [10] requirements, (namely, the energy balance condition, $|\dot{Q}_w - \dot{Q}_{avg}|/\dot{Q}_{avg}$, is less than 0.05, where $\dot{Q}_w$ is the water-side heat transfer rate for $\dot{Q}_w$ and air-side heat transfer rate $\dot{Q}_a$), are considered in the final analysis. Detailed geometry used for the present plain fin-and-tube heat exchangers is tabulated in Table 1. The test fin-and-tube heat exchangers are tension wrapped having a "L" type fin collar. The test conditions of the inlet air are as follows:

Dry-bulb temperatures of the air: 27 ± 0.5 °C
Inlet relative humidity for the incoming air: 50% and 90%
Inlet air velocity: from 0.3 to 3.8 m/s
Inlet water temperature: 7 ± 0.5 °C
Water velocity inside the tube: 1.5–1.7 m/s

The test conditions approximate those encountered with typical fan-coils and evaporators of air-conditioning applications. Uncertainties reported in the present investigation, following the single-sample analysis proposed by Moffat [11], are tabulated in Table 2.

3. Data reduction

3.1. Heat transfer coefficient ($h_{c,o}$)

Basically, the present reduction method is based on the Threlkeld [12] method. Some important reduction procedures of the original Threlkeld method is described as follows:

Table 1
Geometric dimensions of the sample wavy fin-and-tube heat exchangers

No.	Fin thickness (mm)	S_p (mm)	X_f (mm)	D_c (mm)	P_d (mm)	P_t (mm)	P_l (mm)	Row no.
1	0.00012	0.00148	4.7625	0.01038	1.18	0.0254	0.01963	1
2	0.00012	0.00152	4.7625	0.00862	1.58	0.0254	0.02007	1
3	0.00012	0.00270	4.7625	0.01038	1.18	0.0254	0.01963	1
4	0.00012	0.00280	4.7625	0.00862	1.58	0.0254	0.02007	1
5	0.00012	0.00342	4.7625	0.00862	1.58	0.0254	0.02007	1
6	0.00012	0.00351	6.3500	0.00862	1.68	0.0254	0.02627	1
7	0.00012	0.00157	4.7625	0.00862	1.18	0.0254	0.01963	2
8	0.00012	0.00305	4.7625	0.00862	1.18	0.0254	0.01963	2
9	0.00012	0.00159	4.7625	0.00862	1.58	0.0254	0.02007	2
10	0.00012	0.00300	4.7625	0.00862	1.58	0.0254	0.02007	2
11	0.00012	0.00152	4.7625	0.00862	1.58	0.0254	0.02007	4
12	0.00012	0.00158	4.7625	0.00862	1.18	0.0254	0.01963	4
13	0.00012	0.00302	4.7625	0.00862	1.18	0.0254	0.01963	4
14	0.00012	0.00295	4.7625	0.00862	1.58	0.0254	0.02007	4
15	0.00012	0.00145	4.7625	0.01038	1.18	0.0254	0.01963	6
16	0.00012	0.00153	4.7625	0.00862	1.58	0.0254	0.02007	6
17	0.00012	0.00270	4.7625	0.01038	1.18	0.0254	0.01963	6
18	0.00012	0.00294	4.7625	0.00862	1.58	0.0254	0.02007	6

Table 2
Summary of estimated uncertainties

Primary measurements		Derived quantities		
Parameter	Uncertainty	Parameter	Uncertainty $Re_{Dc} = 400$	Uncertainty $Re_{Dc} = 5000$
$\dot{m}_a$	0.3–1%	Re_{Dc}	±1.0%	±0.57%
$\dot{m}_w$	0.5%	Re_{Di}	±0.73%	±0.73%
ΔP	0.5%	$\dot{Q}_w$	±3.95%	±1.22%
T_w	0.05 °C	$\dot{Q}_a$	±5.5%	±2.4%
T_a	0.1 °C	j	±11.4%	±5.9%

The total heat transfer rate used in the calculation is the mathematical average of $\dot{Q}_a$ and $\dot{Q}_w$, namely,

$$\dot{Q}_a = \dot{m}_a(i_{a,in} - i_{a,out}) \tag{1}$$

$$\dot{Q}_w = \dot{m}_w C_{p,w}(T_{w,out} - T_{w,in}) \tag{2}$$

$$\dot{Q}_{avg} = \frac{\dot{Q}_a + \dot{Q}_w}{2} \tag{3}$$

The overall heat transfer coefficient ($U_{o,w}$) based on the enthalpy potential is given as follows:

$$\dot{Q}_{avg} = U_{o,w} A_0 \Delta i_m F \tag{4}$$

where F is the correction factor accounting for a single-pass, cross-flow heat exchanger and Δi_m is the mean enthalpy difference for counter flow coil,

$$\Delta i_m = i_{a,m} - i_{r,m} \tag{5}$$

According to Bump [13] and Myers [14], for the counter flow configuration, the mean enthalpy difference is

$$i_{a,m} = i_{a,in} + \frac{i_{a,in} - i_{a,out}}{\ln\left(\frac{i_{a,in} - i_{r,out}}{i_{a,out} - i_{r,in}}\right)} - \frac{(i_{a,in} - i_{a,out})(i_{a,in} - i_{r,out})}{(i_{a,in} - i_{r,out}) - (i_{a,out} - i_{r,in})} \tag{6}$$

$$i_{r,m} = i_{r,out} + \frac{i_{r,out} - i_{r,in}}{\ln\left(\frac{i_{a,in} - i_{r,out}}{i_{a,out} - i_{r,in}}\right)} - \frac{(i_{r,out} - i_{r,in})(i_{a,in} - i_{r,out})}{(i_{a,in} - i_{r,out}) - (i_{a,out} - i_{r,in})} \tag{7}$$

The overall heat transfer coefficient is related to the individual heat transfer resistance [14] as follows:

$$\frac{1}{U_{o,w}} = \frac{b'_r A_0}{h_i A_{p,i}} + \frac{b'_p A_0 \ln\left(\frac{D_o}{D_i}\right)}{2\pi k_p L_p} + \frac{1}{h_{o,w}\left(\frac{A_{p,o}}{b'_{w,p} A_0} + \frac{A_f \eta_{f,wet}}{b'_{w,m} A_0}\right)} \tag{8}$$

where

$$h_{o,w} = \frac{1}{\frac{C_{p,a}}{b'_{w,m} h_{c,o}} + \frac{y_w}{k_w}} \tag{9}$$

y_w in Eq. (9) is the thickness of the water film. A constant of 0.005 inch was proposed by Myers [14]. In practice, (y_w/k_w) accounts for only 0.5–5% compared to $(C_{p,a}/b'_{w,m} h_{c,o})$, and has often been neglected by previous investigators. As a result, this term is not included in the final analysis.

In this study, we had proposed a more detailed reduction method relative to the conventional lump approach. The proposed method can divide the fin-and-tube heat exchangers into many tiny segments (number of tube rows × number of tube passes per row × number of fins) as shown in Fig. 2. The tube-side heat transfer coefficient, h_i is evaluated from the Gnielinski correlation (Gnielinski, [15]),

$$h_i = \frac{(f_i/2)(Re_{Di} - 1000)Pr}{1.07 + 12.7\sqrt{f_i/2}(Pr^{2/3} - 1)} \cdot \frac{k_i}{D_i} \tag{10}$$

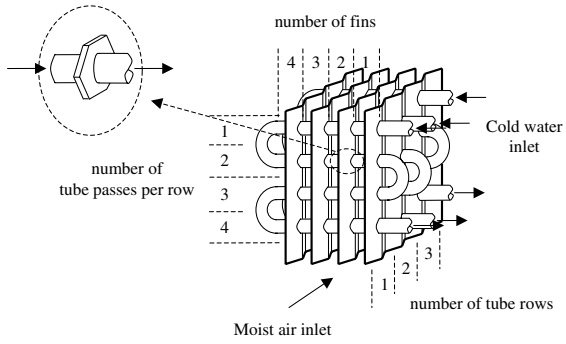

Fig. 2. Dividing of the fin-and-tube heat exchanger into the small pieces.

and the friction factor, f_i is

$$f_i = \frac{1}{(1.58 \ln Re_{Di} - 3.28)^2} \tag{11}$$

The Reynolds number used in Eqs. (10) and (11) is based on the inside diameter of the tube and $Re_{Di} = \rho V D_i/\mu$. In all case, the water side resistance is less than 10% of the overall resistance.

In Eq. (8) there are four quantities ($b'_{w,m}, b'_{w,p}, b'_p$, and b'_r) involving enthalpy-temperature ratios that must be evaluated. The quantities of b'_p and b'_r can be calculated as

$$b'_r = \frac{i_{s,p,i,m} - i_{r,m}}{T_{p,i,m} - T_{r,m}} \tag{12}$$

$$b'_p = \frac{i_{s,p,o,m} - i_{s,p,i,m}}{T_{p,o,m} - T_{p,i,m}} \tag{13}$$

The values of $b'_{w,p}$ and $b'_{w,m}$ are the slope of saturated enthalpy curve evaluated at the outer mean water film temperature at the base surface and the fin surface. Without loss of generality, $b'_{w,p}$ can be approximated by the slope of saturated enthalpy curve evaluated at the base surface temperature [16]. The wet fin efficiency ($\eta_{f,wet}$) based on the enthalpy difference is proposed by Threlkeld [12]. i.e.,

$$\eta_{f,wet} = \frac{i - i_{s,fm}}{i - i_{s,fb}} \tag{14}$$

where $i_{s,fm}$ is the saturated air enthalpy at the mean temperature of fin and $i_{s,fb}$ is the saturated air enthalpy at the fin base temperature. The use of the enthalpy potential equation, greatly simplifies the fin efficiency calculation as illustrated by Kandlikar [17]. However, the original formulation of the wet fin efficiency by Threlkeld [12] was for straight fin configuration (Fig. 3(a)). For a circular fin (Fig. 3(b)), the wet fin efficiency is [16]

$$\eta_{f,wet} = \frac{2r_i}{M_T(r_o^2 - r_i^2)}\left[\frac{K_1(M_T r_i) I_1(M_T r_o) - K_1(M_T r_o) I_1(M_T r_i)}{K_1(M_T r_o) I_0(M_T r_i) + K_0(M_T r_i) I_1(M_T r_o)}\right] \tag{15}$$

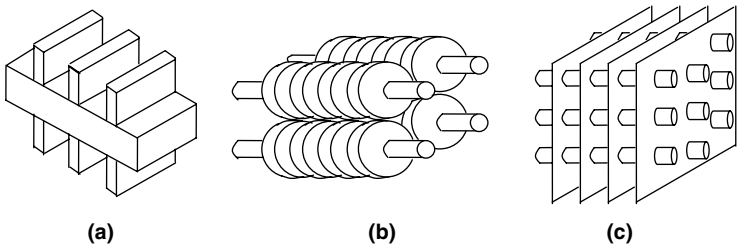

Fig. 3. Type of fin configuration. (a) Straight fin, (b) circular fin, (c) continuous plat fin.

where

$$M_T = \sqrt{\frac{2h_{o,w}}{k_f t}} \tag{16}$$

The test heat exchangers are of Fig. 3(c) configuration. Hence, the corresponding fin efficiency is calculated by the equivalent circular area as depicted by Wang et al. [16]. Evaluation of $b'_{w,m}$ requires a trial and error procedure. For the trial and error procedure, $i_{s,w,m}$ must be calculated using the following equation:

$$i_{s,w,m} = i_{a,m} - \frac{C_{p,a}h_{o,w}\eta_{f,wet}}{b'_{w,m}h_{c,o}} \times \left(1 - U_{o,w}A_0\left[\frac{b'_r}{h_i A_{p,i}} + \frac{b'_p \ln\left(\frac{D_e}{D_i}\right)}{2\pi k_p L_p}\right]\right)(i_{a,m} - i_{r,m}) \tag{17}$$

An algorithm for solving the sensible heat transfer coefficient $h_{c,o}$ for the present row-by-row and tube-by-tube and fin-by-fin reduction method approach is given as follows:

1. Based on the measurement data, calculate the total heat transfer rate $\dot{Q}_{total}$ using Eq. (3).
2. Assume a $h_{c,o}$ for all elements.
3. Calculate the heat transfer performance for each segment with the following procedures.
   - 3.1. Calculate the tube side heat transfer coefficient of h_i using Eq. (10).
   - 3.2. Assume an outlet air enthalpy of the calculated segment.
   - 3.3. Calculate $i_{a,m}$ by Eq. (6) and $i_{r,m}$ by Eq. (7).
   - 3.4. Assume $T_{p,i,m}$ and $T_{p,o,m}$.
   - 3.5. Calculate $\frac{b'_r A_0}{h_i A_{p,i}}$ and $\frac{b'_p A_0 \ln\left(\frac{D_e}{D_i}\right)}{2\pi k_p L_p}$.
   - 3.6. Assume a $T_{w,m}$.
   - 3.7. Calculate the $\eta_{f,wet}$ using Eq. (15).
   - 3.8. Calculate $U_{o,w}$ from Eq. (8).
   - 3.9. Calculate $i_{s,w,m}$ by Eq. (17).
   - 3.10. Calculate $T_{w,m}$ from $i_{s,w,m}$.
   - 3.11. If $T_{w,m}$ derived in step 3.10 is not equal that is assumed in step 3.6, the calculation steps 3.7–3.10 will be repeated with $T_{w,m}$ derived in step 3.10 until $T_{w,m}$ is constant.
   - 3.12. Calculate $\dot{Q}$ of this segment.
   - 3.13. Calculate $T_{p,i,m}$ and $T_{p,o,m}$ from the inside convection heat transfer and the conduction heat transfer of tube and collar.
   - 3.14. If $T_{p,i,m}$ and $T_{p,o,m}$ derived in step 3.13 are not equal that is assumed in step 3.4, the calculation steps 3.5–3.13 will be repeated with $T_{p,i,m}$ and $T_{p,o,m}$ derived in step 3.13 until $T_{p,i,m}$ and $T_{p,o,m}$ are constant.
   - 3.15. Calculate the outlet air enthalpy by Eq. (1) and the outlet water temperature by Eq. (2).
   - 3.16. If the outlet air enthalpy derived in step 3.15 is not equal that is assumed in step 3.2, the calculation steps 3.3–3.15 will be repeated with the outlet air enthalpy derived in step 3.15 until the outlet air enthalpy is constant.
4. If the summation of $\dot{Q}$ for all elements is not equal $\dot{Q}_{total}$, $h_{c,o}$ will be assumed a new value and the calculation step 3 will be repeated until the summation of $\dot{Q}$ for all elements is equal $\dot{Q}_{total}$.

3.2. Mass transfer coefficient ($h_{d,o}$)

For the cooling and dehumidifying of moist air by a cold surface involves simultaneously heat and mass transfer, and can be described by the process line equation from Threlkeld [12]:

$$\frac{di_a}{dW_a} = R\frac{(i_a - i_{s,w})}{(W_a - W_{s,w})} + (i_g - 2501R) \tag{18}$$

where R represent the ratio of sensible heat transfer characteristics to the mass transfer performance,

$$R = \frac{h_{c,o}}{h_{d,o}C_{p,a}} \tag{19}$$

However, for the present fin-and-tube heat exchanger, Eq. (18) did not correctly describe the dehumidification process on the psychrometric chart. This is because the saturated air enthalpy ($i_{s,w}$) at the mean temperature at the fin surface is different from that at the fin base. In

this regard, a modification of the process line on the psychrometric chart corresponding to the fin-and-tube heat exchanger is made. The derivation is as follows:

From the energy balance of the dehumidification one can arrive at the following expression:

$$\dot{m}_a di_a = \frac{h_{c,o}}{C_{p,a}} dA_{p,o}(i_{a,m} - i_{s,p,o,m}) + \frac{h_{c,o}}{C_{p,a}} dA_f(i_{a,m} - i_{s,w,m}) \quad (20)$$

Note that the first term on the right-hand side denotes the heat transfer for the outside tube part whereas the second term is the heat transfer for the fin part. Conservation of water condensate gives

$$\dot{m}_a dW_a = h_{d,o} dA_{p,o}(W_{a,m} - W_{s,p,o,m}) + h_{d,o} dA_f(W_{a,m} - W_{s,w,m}) \quad (21)$$

Dividing Eq. (20) by Eq. (21) yields

$$\frac{di_a}{dW_a} = \frac{R \cdot (i_{a,m} - i_{s,p,o,m}) + R \cdot (\varepsilon - 1) \cdot (i_{a,m} - i_{s,w,m})}{(W_{a,m} - W_{s,p,o,m}) + (\varepsilon - 1) \cdot (W_{a,m} - W_{s,w,m})} \quad (22)$$

where

$$\varepsilon = \frac{A_0}{A_{p,o}} \quad (23)$$

By assuming a value of the ratio of heat transfer to mass transfer, R, and by integrating Eq. (22) with an iterative algorithm, the mass transfer coefficient can be obtained. Analogous procedures for obtaining the mass transfer coefficients are given as

1. Obtain $W_{s,p,o,m}$ and $W_{s,w,m}$ from $i_{s,p,o,m}$ and $i_{s,w,m}$ from those calculation of heat transfer.
2. Assume a value of R.
3. Calculations is performed from the first element to the last element, employing the following procedures:
   3.1. Assume an outlet air humidity ratio.
   3.2. Calculate the outlet air humidity ratio of each element by Eq. (22).
   3.3. If the outlet air humidity ratio obtained from step 3.2 is not equal to the assumed value of step 3.1, the calculation steps 3.1–3.2 will be repeated.
4. If the summation of the outlet air humidity ratio for each element of the last row is not equal to the measured outlet air humidity ratio, assuming a new R value and the calculation step 3 will be repeated until the summation of the outlet air humidity ratio of the last row is equal to the measured outlet air humidity ratio.

3.3. Chilton–Colburn j-factor for heat and mass transfer (j_h and j_m)

The heat and mass transfer characteristics of the heat exchanger is presented by the following non dimensional group:

$$j_h = \frac{h_{c,o}}{G_{max} C_{p,a}} Pr^{2/3} \quad (24)$$

$$j_m = \frac{h_{d,o}}{G_{max}} Sc^{2/3} \quad (25)$$

4. Results and discussion

The heat and mass transfer characteristics of the test samples are in terms of dimensionless parameter j_h and j_m, respectively. Test results were first compared with the original Threlkeld method. The comparison is shown in Fig. 4(a) and (b). For the heat transfer performance, one can see the difference between the original lumped approach is in fair agreement with the present discretized approach. The mean deviation is 10.7%, the dev-

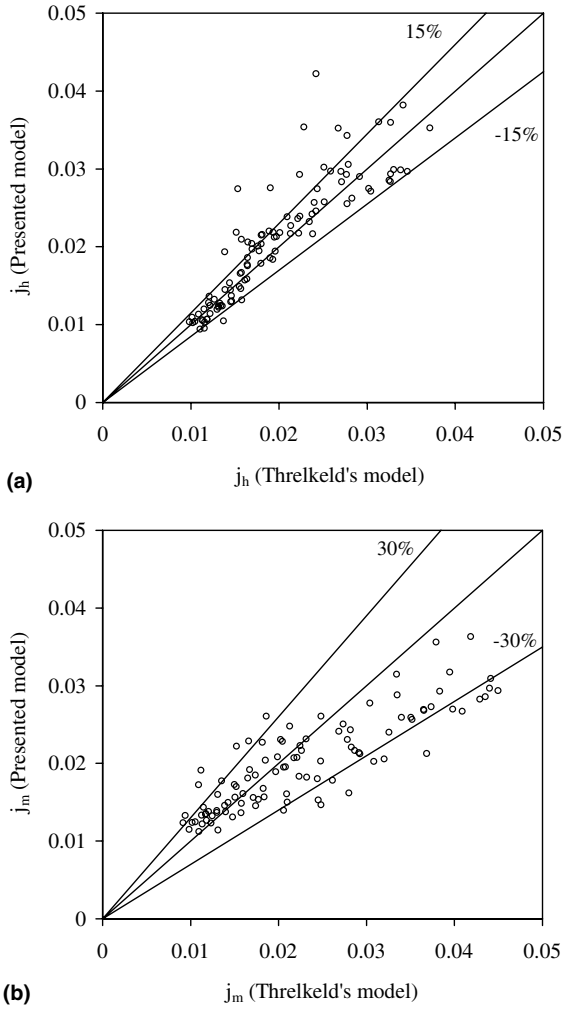

Fig. 4. Comparison of j_h and j_m between those derived by the present method and Threlkeld method. (a) Comparison of j_h and (b) comparison of j_m.

iations lies in larger tube row at RH = 50% where partially dry out occurred on the fin surface. By contrast, for the reduced results of mass transfer performance by the original Threlkeld method, one can see a much larger departure relative to the present reduction method (the mean deviation is 22.9%). This is attributed to the original Threlkeld method is more suitable for counter-cross-flow arrangement and the original method reveals irrational dependence of inlet humidity. A previous study by the present authors [18] had shown an analogous trend for the plain fin geometry under dehumidifying conditions.

The heat and mass transfer performance for 1-row configuration subject to the influence of inlet relative humidity is schematically shown in Fig. 5(a) and (b). As seen in Fig. 5(a), for the same wave height and tube

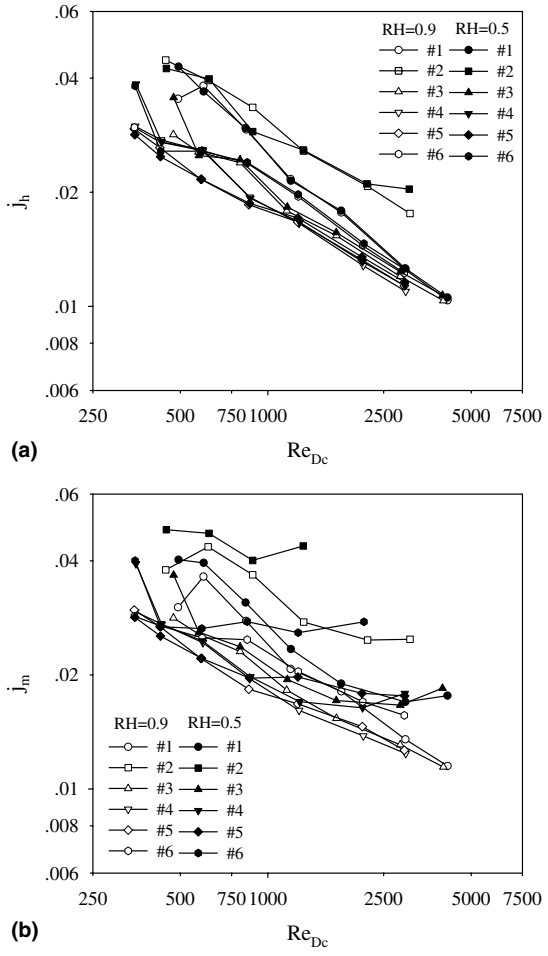

Fig. 5. Influence of relative humidity on the heat and mass transfer performances vs. Re_{Dc} for 1-row configuration. (a) Influence of relative humidity on the heat transfer performance and (b) influence of relative humidity on the mass transfer performance.

diameter (samples #1 and #3), one can see the heat transfer performance for small fin spacing is higher than that having larger fin spacing. The difference becomes especially pronounced at low Reynolds number but is negligible when Re_{Dc} is above 3000. The results are analogous to those tested in fully dry conditions [19]. The phenomenon can be further explained from the numerical results about the effect of fin pitch on the heat transfer performance which was carried out by Torikoshi et al. [20]. They conducted a 3-D numerical investigation of a 1-row plain fin-and-tube heat exchanger. Their investigation shows that the vortex forms behind the tube can be suppressed and the entire flow region can be kept steady and laminar when the fin pitch is small enough. Further increase of fin pitch would result in a noticeable increase of cross-stream width of vortex region behind the tube. As a result, lower heat transfer performance is seen for larger spacing. In the meantime, the difference vanishes when Re_{Dc} is above 3000, this is attributed to the change of flow pattern into vortex dominated region. Note that their simulations also showed that higher velocity may result in the occurrence of vortex along the fins, therefore the effect of fin pitch on heat transfer coefficient would be negligible.

In Fig. 5(a), one can also examine the influence of wave height on the heat transfer performance. At a larger fin spacing (samples #3 and #4), the effect of wave height on heat transfer performance is relatively small. In fact, for a wide spacing of 2.7–2.8 mm, the effect of wave height is negligible whether P_d is 1.18 mm or 1.58 mm. Nevertheless, one can see the effect of wave height on heat transfer performance is rather noteworthy at a smaller fin spacing (sample #2). The results are analogous to those tested in dry conditions [3–5]. Based on the simulation results by Ramadhyani [21] and Jang and Chen [22], Wang et al. [23] pointed out appreciable increase of heat transfer coefficients can be obtained only when the corrugation angle is larger than 20°. Hence, compared to the present results in wet condition, it seems that this finding is still applicable to the test results under dehumidifying conditions. In Fig. 5(a), the influence of relative humidity on heat transfer performance is rather small, the results are in line with previous studies [16,7].

The effect of inlet relative humidity on the mass transfer characteristics is shown in Fig. 5(b). Similarly, the influence of inlet relative humidity is rather small when the fin spacing is sufficiently large (>2.0 mm, samples #3, #5, and #6). However, at a smaller fin spacing (samples #1, #2) one observe a slight decrease of j_m when the inlet relative humidity is increased from 50% to 90%. The slight decrease of mass transfer performance with inlet relative humidity at dense fin spacing may be associated with the condensate retention phenomenon. Yoshii et al. [24] conducted a flow pattern observation about the air flow across tube bank, their

results indicate the blockage of the tube row by the condensate retention may hinder the performance of the heat exchangers. Thus one can see a slight drop of mass transfer performance. However, a considerable increase of mass transfer performance when $RH = 0.5$ and $Re_{Dc} > 1000$ is encountered. This is attributed to the blow-off condensate by flow inertia which makes more zoom for water vapor to condense along the surface.

The aforementioned results are applicable for the 1-row configurations, test results for the 2-rows configuration is shown in Fig. 6(a) and (b). For the heat transfer performance shown in Fig. 6(a), one can see the performance difference is reduced regardless the influences are from inlet relative humidity, P_d, or from fin spacing. With the increase of the number of tube rows, the condensate blow-off phenomenon in the row is blocked by

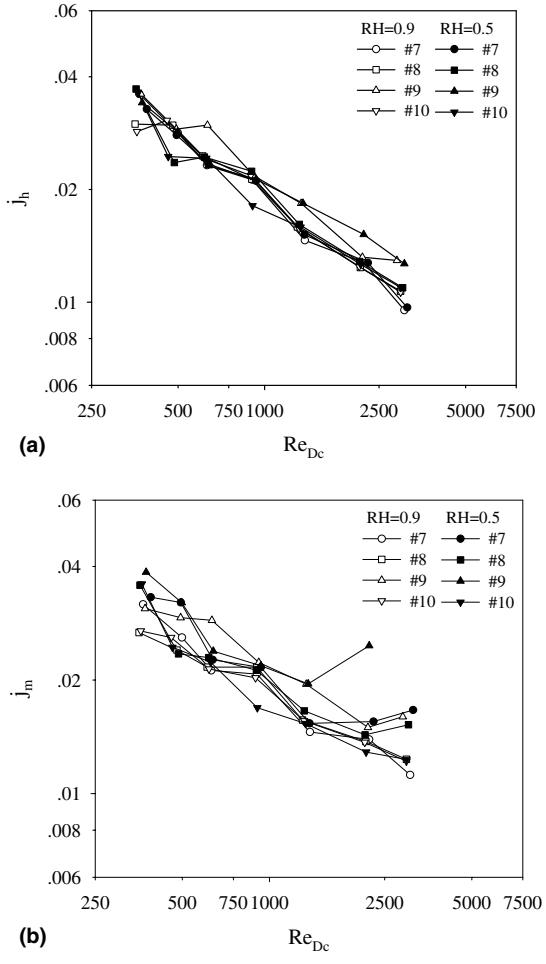

Fig. 6. Influence of relative humidity on the heat and mass transfer performances vs. Re_{Dc} for 2-row configuration. (a) Influence of relative humidity on the heat transfer performance and (b) influence of relative humidity on the mass transfer performance.

the subsequent row. In that regard, the influence of relative humidity on the mass transfer performance becomes less profound and is deferred to a even higher Reynolds number ($Re_{Dc} > 2000$). Analogous results (the influence of relative humidity, P_d, and fin spacing on the heat and mass transfer performance) are obtained when the number of tube rows is further increased to 4 or 6. The results agree with those reported by Wang et al. [16]. They reported negligible influence of fin pitch and inlet conditions on the heat transfer performance of a plain fin geometry when $N = 4$. The decrease of geometrical influences on the heat and mass transfer with the rise number of tube rows can be made more clear from a previous flow visualization study using scale-up fin-and-tube heat exchangers [25]. Their flow visualization experiment shows the injected dye in front of the first tube row hits the round tube and twists and swirls to the subsequent row. A clear horseshoe vortex is shown in front of the tube. The strength of the vertical motion is apparently stronger near the first row when comparing to the second and third row. The strength of swirled motion decays markedly with increasing row. As a consequence, the associated influences of geometries becomes less profound.

The dehumidifying process involves heat and mass transfer simultaneously, if mass transfer data are unavailable, it is convenient to employ the analogy between heat and mass transfer. The existence of the heat and mass analogy is because the fact that conduction and diffusion in a liquid are governed by physical laws of identical mathematical form. Therefore, for air-water vapor mixture, the ratio of $h_{c,o}/h_{d,o}C_{p,a}$ is generally around unity, i.e.

$$\frac{h_{c,o}}{h_{d,o}C_{p,a}} \approx 1 \tag{26}$$

The term in Eq. (26) approximately equals to unity for dilute mixtures like water vapor in air near the atmospheric pressure (temperature well-below corresponding boiling point). The validity of Eq. (26) relies heavily on the mass transfer rate. The experimental data of Hong and Webb [26] indicated that this value is between 0.7 and 1.1, Seshimo et al. [27] gave a value of 1.1. Eckels and Rabas [28] also reported a similar value of 1.1–1.2 for their test results of plain fin-and-tube heat exchangers. The aforementioned studies all showed the applicability of Eq. (26). In the present study, we notice that the values of $h_{c,o}/h_{d,o}C_{p,a}$ were generally between 0.6 and 1.1 (shown in Fig. 7) which indicates the analogy is roughly applicable. However, the present authors found that the analogy is not applicable using the original Threlkeled method (the ratio is from 0.5–2.2). There are two differences between the original Threlkeld method and the present row-by-row and tube-by-tube approach. Firstly, larger deviation occurs via using the original Threlkeled's methods. This is associated with

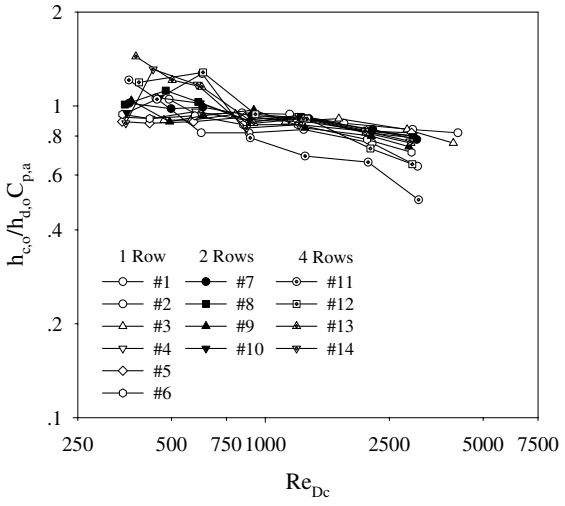

Fig. 7. $h_{c,o}/h_{d,o}C_{p,a}$ plotted against Re_{Dc}.

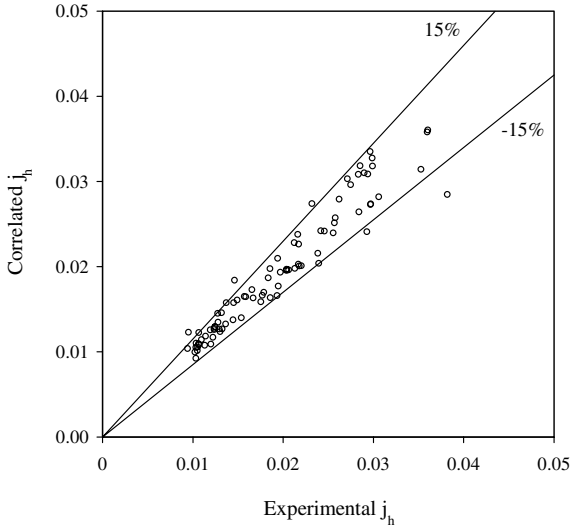

Fig. 8. Comparison of j_h between those derived by correlation and experiment.

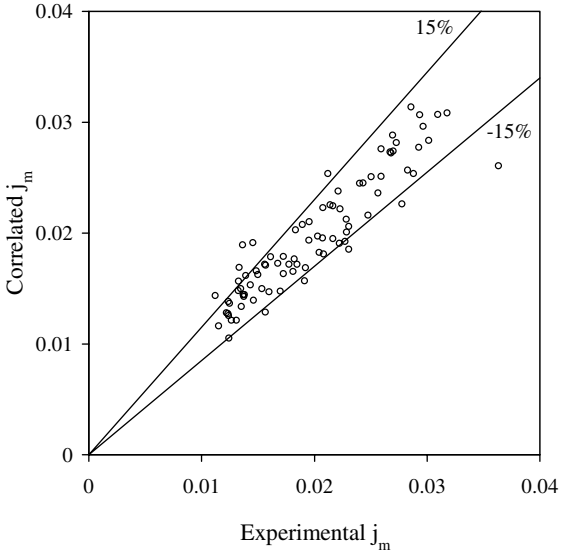

Fig. 9. Comparison of j_m between those derived by correlation and experiment.

the considerable influence of inlet humidity of the original Threlkeld's method whereas for the present reduction method, the ratio is relatively insensitive to change of inlet humidity provided that the surface is fully wet. Secondly, reduction by the present method indicates that the ratio of $h_{c,o}/h_{d,o}C_{p,a}$ is slightly decreased with the rise of Reynolds number whereas the original Threlkeld method shows the opposite trend (slightly increases with the Reynolds number). As aforementioned in previous section, with the rise of inlet flow inertia, the condensate can be easily removed for making more room for further condensation. The condensate removal becomes even pronounced with smaller fin spacing. In that regard, the removal of condensate subject to larger flow inertia help to improve the mass transfer performance. Therefore, one can see the ratio of $h_{c,o}/h_{d,o}C_{p,a}$ is slightly decreased with the fin spacing. Notice that the effect of fin spacing on the ratio of $h_{c,o}/h_{d,o}C_{p,a}$ is also insignificant. This is associated with the high air flow rate would increase the vapor shear, and wipe away the condensate that leads to increase heat and mass transfer simultaneously. Therefore, the effect of fin spacing on the ratio of $h_{c,o}/h_{d,o}C_{p,a}$ is comparatively small.

Based on previous discussions, there is not single curve that can describe the phenomena for both j_h and j_m. In that regard, we had performed a multiple regression technique in a practical range of experimental data ($300 < Re_{Dc} < 4500$) to generate design correlations, the appropriate correlation form of j_h and j_m for the present data are as follows:

$$j_h = 0.171\varepsilon^{0.377N} Re_{D_c}^{(-0.0142N-0.478)} \left(\frac{Sp}{D_c}\right)^{(0.00412N-0.0217)} \times \left(\frac{A_0}{A_{p,o}}\right)^{(-0.114N+0.440)} \quad (27)$$

$$j_m = 0.315\varepsilon^{0.441N} Re_{D_c}^{(0.0580N-0.475)} \left(\frac{Sp}{D_c}\right)^{(-0.00471N+0.0216)} \times \left(\frac{A_0}{A_{p,o}}\right)^{(0.00223N+0.223)} \quad (28)$$

$$\frac{h_{c,o}}{h_{d,o}C_{p,a}} = 0.490\varepsilon^{0.792N} Re_{D_c}^{(-0.0714N+0.00361)} \left(\frac{Sp}{D_c}\right)^{(0.00867N-0.0425)} \times \left(\frac{A_0}{A_{p,o}}\right)^{(-0.107N+0.203)} \quad (29)$$

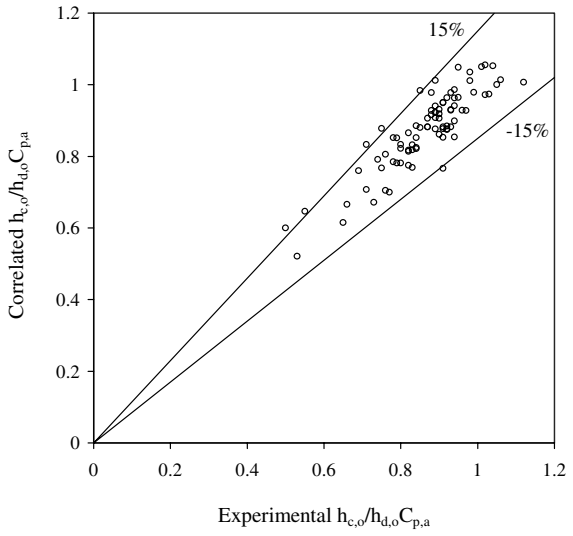

Fig. 10. Comparison of $h_{c,o}/h_{d,o}C_{p,a}$ between those derived by correlation and experiment.

As shown in Figs. 8–10, Eq. (27) can describe 94.19% of j_h within 15%, Eq. (28) can describe 83.72% of j_m within 15%, and Eq. (29) can describe 93.02% of $h_{c,o}/h_{d,o}C_{p,a}$ within 15%.

5. Conclusions

The present study examines the heat and mass transfer characteristics of 18 wavy fin-and-tube heat exchangers under dehumidifying conditions. On the basis of the results and discussions, the following results are concluded:

1. A new reduction method based on the Threlkeld method is proposed in this study for reducing the test results. For fully wet conditions, the sensible heat transfer characteristic and mass transfer characteristic by the present method are relatively insensitive to the inlet relative humidity.
2. For fully wet conditions having 1-row configuration, the heat transfer performance and mass transfer performance shows appreciable influence of fin spacing. Both the heat transfer performance is increased when the fin spacing is reduced. However, the difference becomes less noticeable when $Re_{Dc} > 3000$. The influence is also related to the wave height, larger wave height shows much larger difference with the fin spacing. Moreover, both j_h and j_m are comparatively independent of the fin spacing when the number of tube rows is increased (e.g. $N > 2$).
3. The effect of inlet conditions and geometrical parameters on the heat and mass performance becomes less significant with the number of tube rows.
4. The ratio of $h_{c,o}/h_{d,o}C_{p,a}$ is in the range 0.6–1.1 and is insensitive to change of fin spacing.
5. The correlations are proposed for the wavy fin-and-tube heat exchangers. These correlations can describe 94.19% of the j_h factors within 15%, can describe 83.72% of the j_m factors within 15%, and can describe 93.02% of the ratio $h_{c,o}/h_{d,o}C_{p,a}$ of within 15%.

Acknowledgement

The authors are indebted to the Thailand Research Fund (TRF) and the Energy R&D foundation funding from the Bureau of Energy of the Ministry of Economic Affairs, Taiwan for supporting this study.

References

[1] D.T. Beecher, T.J. Fagan, Effects of fin pattern on the air-side heat transfer coefficient in plate finned-tube heat exchanger, ASHRAE Trans. 93 (2) (1987) 1961–1984.
[2] W.M. Yan, P.J. Sheen, Heat transfer and friction characteristics of fin-and-tube heat exchangers, Int. J. Heat Mass Transfer 43 (2000) 1651–1659.
[3] C.C. Wang, W.L. Fu, C.T. Chang, Heat transfer and friction characteristics of typical wavy fin-and-tube heat exchangers, Exp Thermal Fluid Sci. 14 (2) (1997) 174–186.
[4] C.C. Wang, Y.M. Tsi, D.C. Lu, Comprehensive study of convex-louver and wavy fin-and-tube heat exchangers, AIAA J. Thermophys. 12 (3) (1998) 423–430.
[5] C.C. Wang, Y.T. Lin, C.J. Lee, Investigation of wavy fin-and-tube heat exchangers: a contribution to data bank, Exp. Heat transfer 12 (1999) 73–89.
[6] C.C. Wang, Y.M. Hwang, Y.T. Lin, Empirical correlations for heat transfer and flow friction characteristics of herringbone wavy fin-and-tube heat exchangers, Int. J. Refrig. 25 (2002) 673–680.
[7] Y.T. Lin, Y.M. Hwang, C.C. Wang, Performance of the herringbone wavy fin under dehumidifying conditions, Int. J. Heat Mass Transfer 45 (2002) 5035–5044.
[8] ASHRAE Standard 41.2-1987, Standard Methods for Laboratory Air-Flow Measurement, American Society of Heating, Refrigerating and Air-Conditioning Engineers Inc., Atlanta GA, 1987.
[9] ASHRAE Standard 41.1-1986, Standard Method for Temperature Measurement, American Society of Heating, Refrigerating and Air-Conditioning Engineers, Inc., Atlanta, GA, 1986.
[10] ASHRAE Standard, Method of Testing Forced Circulation Air Cooling and Air Heating Coils, American Society of Heating, Refrigerating and Air-Conditioning Engineers, Inc., Atlanta, GA, 1978, pp. 33–78.
[11] R.J. Moffat, Describing the uncertainties in experimental results, Exp. Thermal Fluid Sci. 1 (1988) 3–17.
[12] J.L. Threlkeld, Thermal Environmental Engineering, Prentice-Hall, Inc., New-York, NY, 1970.
[13] T.R. Bump, Average temperatures in simple heat exchangers, ASME J. Heat Transfer 85 (2) (1963) 182–183.

[14] R.J. Myers, The effect of dehumidification on the air-side heat transfer coefficient for a finned-tube coil, M.S. Thesis, University of Minnesota, Minneapolis, 1967.
[15] V. Gnielinski, New equation for heat and mass transfer in turbulent pipe and channel flow, Int. Chem. Eng. 16 (1976) 359–368.
[16] C.C. Wang, Y.C. Hsieh, Y.T. Lin, Performance of plate finned tube heat exchangers under dehumidifying conditions, J. Heat Transfer 119 (1997) 109–117.
[17] S.G. Kandlikar, Thermal design theory for compact evaporators, in: R.K. Kraus et al. (Eds.), Compact Heat Exchangers, Hemisphere Publishing Corp., New York, NY, 1990, pp. 245–286.
[18] W. Pirompugd, S. Wongwises, C.C. Wang, A tube-by-tube reduction method for simultaneous heat and mass transfer characteristics for plain fin-and-tube heat exchangers in dehumidifying conditions, Heat Mass Transfer 41 (8) (2005) 756–765.
[19] C.C. Wang, K.U. Chi, Heat transfer and friction characteristics of plain fin-and-tube heat exchangers: Part I: new experimental data, Int. J. Heat Mass Transfer 43 (2000) 2681–2691.
[20] K. Torikoshi, G. Xi, Y. Nakazawa, H. Asano, Flow and heat transfer performance of a plate-fin and tube heat echanger (1st report: effect of fin pitch), in: 10th International Heat Transfer Conf. (1994), paper 9-HE-16 411-416.
[21] S. Ramadhyani, Numerical prediction of flow and heat transfer in corrugated ducts, ASME paper, HTD, vol. 66, 1986, pp. 37–43.
[22] J.Y. Jang, L.K. Chen, Numerical analysis of heat transfer and fluid flow in a three-dimensional wavy-fin and tube heat exchanger, Int. J. Heat Mass Transfer 40 (1997) 3981–3990.
[23] C.C. Wang, J.Y. Jang, N.F. Chiou, Effect of waffle height on the air-side performance of wavy fin-and-tube heat exchangers, Heat Transfer Eng. 20 (3) (1999) 45–56.
[24] T. Yoshii, M. Yamamoto, M. Otaki, Effects of dropwise condensate on wet surface heat transfer of air cooling coils, in: Proceedings of the 13th International Congress of Refrigeration, 1973, pp. 285–292.
[25] C.C. Wang, J. Lo, Y.T. Lin, C.S. Wei, Flow visualization of annular and delta winglet vortex generators in fin-and-tube heat exchanger application, Int. J. Heat Mass Transfer 45 (2002) 3803–3815.
[26] T.K. Hong, R.L. Webb, Calculation of fin efficiency for wet and dry fins, Int. J. HVAC & R Res 2 (1) (1996) 27–41.
[27] Y. Seshimo, K. Ogawa, K. Marumoto, M. Fujii, Heat and mass transfer performances on plate fin and tube heat exchangers with dehumidification, Trans. JSME 54 (499) (1988) 716–721.
[28] P.W. Eckels, T.J. Rabas, Dehumidification: on the correlation of wet and dry transport process in plate finned-tube heat exchangers, ASME J. Heat Transfer 109 (1987) 575–582.